# Nonequilibrium charge recombination from the excited adiabatic state of donor-acceptor complexes

Valentina A. Mikhailova and Anatoly I. Ivanov[a)]
*Department of Physics, Volgograd State University, 2nd Prodolnaya Street, 30, Volgograd 400062, Russia*

Eric Vauthey
*Department of Physical Chemistry, University of Geneva, 30 Quai Ernest Ansermet, CH-1211 Geneva 4, Switzerland*

(Received 21 May 2004; accepted 14 July 2004)

A model of nonequilibrium charge recombination from an excited adiabatic state of a donor-acceptor complex induced by the nonadiabatic interaction operator is considered. The decay of the excited state population prepared by a short laser pulse is shown to be highly nonexponential. The influence of the excitation pulse carrier frequency on the ultrafast charge recombination dynamics of excited donor-acceptor complexes is explored. The charge recombination rate constant is found to decrease with increasing excitation frequency. The variation of the excitation pulse carrier frequency within the charge transfer absorption band of the complex can alter the effective charge recombination rate by up to a factor 2. The magnitude of this spectral effect decreases strongly with increasing electronic coupling. © *2004 American Institute of Physics.*
[DOI: 10.1063/1.1789940]

## I. INTRODUCTION

The charge recombination (CR) dynamics of excited donor-acceptor complexes (DACs) or contact ion pairs exhibit several specific features, such as the absence of the normal region predicted by Marcus theory. Indeed, the CR rate constant exhibits a monotonous, nearly exponential, decrease with increasing reaction exergonicity over a very wide interval going from $-0.5$ eV up to $-3$ eV.[1–4] An explanation for such an unexpected dependence of the rate has been proposed in Ref. 5. It is based on the fact that the laser excitation populates a nonequilibrium initial vibrational state of the DAC. Therefore, in the low driving force regime, where the normal behavior is predicted, CR proceeds in parallel to solvent relaxation, and consequently the excited state population decays before being trapped in the equilibrium configuration. The calculations performed within the framework of the stochastic point-transition approach[6,7] could well reproduce the experimentally observed free energy dependence of the rate.[5] There are, however, two problems in this explanation.[8] First, a good fit requires too large electronic coupling values and therefore the diabatic state representation and the stochastic approach, which is based on it, are no longer applicable. Second, this model predicts a strong time dependence of the rate constant, in disagreement with most experimental data.[1–4]

More recently, a model considering the CR of excited DACs as a transition between excited and ground adiabatic states induced by the nonadiabatic interaction has been proposed.[8] Such a perturbation theory in the nonadiabatic interaction had been developed earlier in Ref. 9 within the framework of the semiclassical theory. With the assumption that the time scale of nuclear relaxation is much shorter than that of CR, the authors could very well reproduce the experimentally observed free energy dependence of the rate constant. Moreover, both above-mentioned problems are no longer present in this model. Indeed, it can be applied to systems with a strong electronic coupling and it predicts an exponential CR dynamics.

However, the time scales associated to solvent relaxation, or at least some of them, are often slower than that of CR. Therefore, a theoretical model for the description of ultrafast electron transfer (ET) dynamics has to consider the time dependence of the CR rate constant. This issue has been investigated intensively over the last decade. An expression for the population decay from an electronic state initially prepared with a nonequilibrium nuclear distribution has been derived in Ref. 10. The importance for electron transfer of the optical preparation of a nonequilibrium nuclear distribution on the donor state has also been shown.[11] Nonequilibrium effects on ultrafast ET dynamics, with a special emphasis on vibrational coherence, have been explored using nonperturbative methods in electronic coupling.[12–15] The role of vibrational coherence in ultrafast electron transfer reactions has been discussed in detail in Ref. 16. The hybrid model proposed in Ref. 17 accounting for nonequilibrium population of the initial vibrational state has been used successfully to describe the free energy dependence of the CR rate of excited DACs.[4]

The dependence of the CR rate of DACs on the pump pulse carrier frequency, the so-called spectral effect, observed recently[18,19] opens promising perspectives for the investigation of subtle features connected to ultrafast electron transfer reactions. Indeed, the spectral effect reflects explicitly the nonstationarity of the nuclear subsystem during CR and can thus only be understood within the framework of a

a)Author to whom correspondence should be addressed. Electronic mail: physic@vlink.ru

 

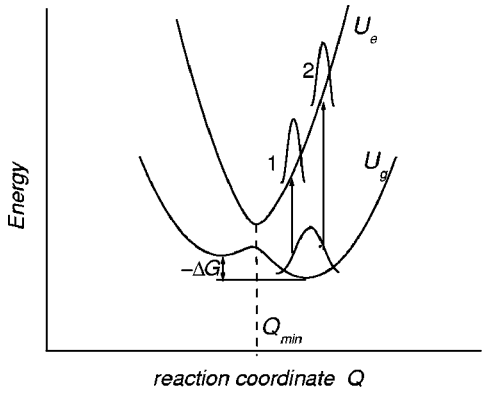


FIG. 1. Adiabatic free energy curves for the ground $U_g$ and excited $U_e$ electronic states. The optical excitation of the system is represented by the arrows with the length proportional to the excitation frequency. The numbers 1 and 2 represent the initial locations of the wave packet in the excited state.

nonstationary model. The theory of the spectral effect in the weak electronic coupling limit has been developed in Ref. 20. The magnitude of the spectral effect was shown to depend strongly on both the CR free energy and the dynamic properties of the medium.

The aim of this paper is to investigate theoretically the influence of the vibrational nonstationarity and of the carrier frequency of the excitation pulse on the ultrafast CR dynamics of excited DACs. For this purpose, the model presented in Ref. 8 is generalized to the case of nonstationary CR, where the initial nonequilibrium vibrational state depends explicitly on the excitation pulse characteristics. Generally, vibrational nonequilibrium is expected to lead to strong nonexponential CR kinetics. The conditions where the CR dynamics become nearly exponential in the experimentally observable time window are also investigated.

## II. NONSTATIONARY ADIABATIC PERTURBATION THEORY

The photoexcitation of a DAC results in the population, a state with a strong charge transfer character, which is often considered as a contact ion pair. In polar solvents, this ion pair can either dissociate into free ions or return radiatively or nonradiatively to the ground state. In many DACs, nonradiative CR, which is later on assumed to be the only deactivation pathway of excited DACs, dominates.[1,21–25] The model considers CR of excited DACs as a two-state problem with the ground and excited adiabatic electronic states of the complex. A laser pulse is assumed to produce an initial nonequilibrium population on the free energy surface of the excited state, as shown in Fig. 1. The Hamiltonian of the system in the adiabatic representation can be written as[9,26]

$$H=\begin{pmatrix} H_e & V_n \\ V_n^+ & H_g \end{pmatrix}, \tag{1}$$

where $V_n=-i[P,C(Q)]_+/2$ is the nonadiabatic interaction operator;

$$H_e=\frac{P^2}{2M}+\frac{M\Omega^2Q^2}{2}+\frac{1}{2}\Omega_{\mathrm{ad}}(Q)+H_m, \tag{2}$$

$$H_g=\frac{P^2}{2M}+\frac{M\Omega^2Q^2}{2}-\frac{1}{2}\Omega_{\mathrm{ad}}(Q)+H_m, \tag{3}$$

$H_g$ and $H_e$ are the vibrational Hamiltonian of the ground and excited adiabatic states, respectively, and $H_m$ is the Hamiltonian of the bath including its interaction with the reaction coordinate. The parameters $M$ and $\Omega$ are expressed in terms of the spectral density of the bath oscillators $J(\omega)$,[27]

$$\frac{1}{2M}=E_r\Omega^2=\int_0^\infty J(\omega)\omega d\omega. \tag{4}$$

In this equation and in the following, the Planck constant $\hbar$ is set to unity. The reorganization energy $E_r$ is given by

$$E_r=\frac{1}{\pi}\int_0^\infty \frac{J(\omega)}{\omega}d\omega.$$

The quantity $\Omega_{\mathrm{ad}}(Q)$ is the free energy gap between the adiabatic states,

$$\Omega_{\mathrm{ad}}(Q)=\sqrt{(Q-\Delta G)^2+4V_{\mathrm{el}}^2}, \tag{5}$$

where $\Delta G$ is the CR free energy. The coefficient $C$ has the following form:

$$C(Q)=\frac{V_{\mathrm{el}}}{M\Omega_{\mathrm{ad}}^2(Q)}.$$

The temporal evolution of the system considered is described by the quantum Liouville equation for the density operator $\varrho$:

$$i\frac{\partial\varrho}{\partial t}=[H,\varrho].$$

The vibrational population is assumed to be initially in thermal equilibrium in the adiabatic ground state (see Fig. 1). Then a short pump pulse, centered at time $t=0$, transfers the population to the excited adiabatic state. The initial population of the excited adiabatic state $\varrho_{\mathrm{ee}}(0)$ depends on the pump pulse characteristics and will be determined later.

Using these initial conditions and applying the standard methods of time-dependent perturbation theory (see, for examples, Refs. 10, 28, and 29) in the nonadiabatic interaction $V_n$, we obtain the reaction rate $k(t)$ in the first nonvanishing order

$$k(t)=\int_0^t \mathrm{Tr}\{e^{iH_e(t-t_1)}V_n e^{-iH_g(t-t_1)}V_n^+\varrho_{\mathrm{ee}}(t_1)+\mathrm{h.c.}\}dt_1, \tag{6}$$

where

$$\varrho_{\mathrm{ee}}(t)=e^{-iH_e t}\varrho_{\mathrm{ee}}(0)e^{iH_e t},$$

h.c. is the Hermitian conjugate. The time dependence $\varrho_{\mathrm{ee}}(t)$ reflects the propagation of the wave packet on the excited state free energy surface.

Considerable simplification of Eq. (6) is achieved if the motion along the reaction coordinate within the time scale of momentum relaxation can be neglected (strong friction limit).[8]

This immediately leads to the following equation:

$$e^{-iH_g(t-t_1)}\simeq e^{-iH_e(t-t_1)}e^{i\Omega_{\mathrm{ad}}(Q)(t-t_1)}. \tag{7}$$

Tracing over all bath coordinates except that of reaction results to the following reaction rate:

$$k(t)=\frac{1}{2\pi}\int_0^t dt_1\int_{-\infty}^{\infty}dQ\int_{-\infty}^{\infty}d\omega R(\omega)C^2(Q) \times e^{i(\Omega_{\mathrm{ad}}-\omega)(t-t_1)}\varrho_{\mathrm{ee}}(Q,t_1)+\mathrm{c.c.}, \tag{8}$$

where $\varrho_{\mathrm{ee}}(Q,t)$ is the diagonal element of the reduced density matrix in the coordinate representation of the excited adiabatic state and c.c. is the complex conjugate. $R(\omega)$ is the Fourier transform of the momentum correlation function

$$\langle e^{iH_e t}Pe^{-iH_e t}P\rangle=\frac{1}{2\pi}\int_{-\infty}^{\infty}R(\omega)e^{-i\omega t}d\omega \tag{9}$$

and can be expressed in terms of the spectral density $J(\omega)$,[30,31]

$$R(\omega)=M^2\omega^2 J(\omega)\left[\coth\left(\frac{\omega}{2k_BT}\right)+1\right], \tag{10}$$

where $k_B$ is the Boltzmann constant and $T$ is the temperature.

Substitution of Eq. (10) into Eq. (8) results in the final expression for the time-dependent rate

$$k(t)=V_{\mathrm{el}}^2\int_{-\infty}^{\infty}dQ\int_0^t dt_1\frac{\varrho_{\mathrm{ee}}(Q,t_1)}{\Omega_{\mathrm{ad}}^4(Q)}g(Q,t-t_1), \tag{11}$$

where

$$g(Q,t-t_1)=\frac{1}{\pi}\int_{-\infty}^{\infty}d\omega\omega^2 J(\omega)\cos\{[\Omega_{\mathrm{ad}}(Q)-\omega](t-t_1)\} \times\left[\coth\left(\frac{\omega}{2k_BT}\right)+1\right]. \tag{12}$$

Equation (11) describes the CR dynamics occurring in parallel to vibrational relaxation. As the vibrational subsystem is approaching thermal equilibrium, the rate $k(t)$ is approaching the stationary value $k_{\mathrm{st}}$. Indeed, the function $g(Q,t)$ decays within the time scale of momentum relaxation. Therefore, for time larger than the time scale related to the relaxation of the reaction coordinate, one can set in the integral (11) $\varrho_{\mathrm{ee}}(Q,t_1)\simeq\varrho_{\mathrm{ee}}^{\mathrm{eq}}(Q)$, where

$$\varrho_{\mathrm{ee}}^{\mathrm{eq}}(Q)=\frac{e^{-U_e/k_BT}}{\mathrm{Tr}\,e^{-U_e/k_BT}}$$

is the equilibrium coordinate distribution on the adiabatic excited state potential $U_e$,

$$U_e=\frac{Q^2}{4E_r}+\frac{1}{2}\Omega_{\mathrm{ad}}(Q). \tag{13}$$

Integrating Eq. (11) over time and using the representation of the $\delta$ function

$$\lim_{t\to\infty}\frac{\sin\omega t}{\omega}=\pi\delta(\omega)$$

yields the stationary rate constant

$$k_{\mathrm{st}}=k(t\to\infty)=V_{\mathrm{el}}^2\int_{-\infty}^{\infty}dQ\frac{\varrho_{\mathrm{ee}}^{\mathrm{eq}}(Q)}{\Omega_{\mathrm{ad}}^2(Q)}J[\Omega_{\mathrm{ad}}(Q)] \times\left[\coth\left(\frac{\Omega_{\mathrm{ad}}(Q)}{2k_BT}\right)+1\right], \tag{14}$$

which corresponds to the original result of Ref. 8.

## III. WAVE PACKET DYNAMICS

To find out the initial vibrational state population, $\varrho_{\mathrm{ee}}(Q,0)$, we consider the dipole interaction between the DAC and the laser pulse

$$V_{\mathrm{dip}}(t)=-\langle e|\vec{d}\vec{E}(t)|g\rangle,$$

where $\vec{d}$ is the transition dipole moment and $\vec{E}(t)$ is the electric pump field. The optical coupling operator can be expressed as

$$V_{\mathrm{dip}}(t)=V_0\exp(-i\omega_e t-t^2/\tau_e^2).$$

The pump pulse is thus only determined by two parameters, namely, the carrier frequency $\omega_e$ and the duration $\tau_e$. The pump pulses are assumed to be transform limited and their intensity spectrum $I(\omega)$ is given by

$$I(\omega)\sim\exp[-(\omega-\omega_e)^2\tau_e^2/2].$$

If the duration of the pulse is shorter than the nuclear dynamics time scales, excited state dynamics during excitation can be neglected. In this case, the initial shape of the wave packet on the excited surface, $\varrho_{\mathrm{ee}}(Q,t=0)$, is determined by the product of the initial nuclear distribution in the ground state and the excitation pulse spectrum, that is,

$$\varrho_{\mathrm{ee}}(Q,t=0)=Z^{-1}\exp\left\{-\frac{U_g(Q)}{k_BT}\right\} \times\exp\left\{-\frac{[U_e(Q)-U_g(Q)-\omega_e]^2\tau_e^2}{2}\right\}, \tag{15}$$

where $Z$ is a normalization factor and

$$U_g=U_e-\Omega_{\mathrm{ad}}(Q) \tag{16}$$

is the free energy of the adiabatic ground state.

From Eq. (15), it follows that if the spectral width of the excitation pulse is much smaller than the absorption bandwidth, the coordinate of the wave packet maximum is determined by the equation

$$\Omega_{\mathrm{ad}}(Q)=\omega_e. \tag{17}$$

To simplify the calculations, the wave packet propagation is approximated by

$$\varrho_{\mathrm{ee}}(Q,t)=Z^{-1}\exp\left\{-\frac{U_e\{Q-[Q(t)-Q_{\mathrm{min}}]\}}{k_BT\delta(t)}\right\}, \tag{18}$$

where $Q_{\mathrm{min}}$ is the location of the excited surface minimum and $\delta(0)=1-A=B\tau_e^{-2}$ is the initial width of the wave packet. The parameters $A$ and $B$ are complex functions of the magnitude of $E_r$, $V_{\mathrm{el}}$, $\Delta G$, and $k_BT$. The expressions for $A$ and $B$ are not written explicitly because, in the range of parameters considered here, the electron transfer kinetics de-

pends only weakly on the initial wave packet width. The function $Q(t)$ describes the time-dependent position of the wave packet maximum, and its initial value $Q(0)$ is the solution of Eq. (17). It should be noted that Eq. (18) gives a correct maximum position and width of the initial wave packet, but a slightly distorted shape.

The propagation of the wave packet is approximated by Eq. (18) that requires the knowledge of the functions $Q(t)$ and $\delta(t)$. It is well known that these functions are directly connected to various phenomena such as, for example, the time dependence of fluorescence spectra.[32–34] Indeed, the function $Q(t)$ determines the time-dependent Stokes shift because $\Omega_{\mathrm{ad}}[Q(t)]$ is equal to the frequency of the fluorescence maximum. Therefore a relationship between $Q(t)$ and the experimentally measurable time-dependent Stokes shift can be established[34]

$$X(t)=\frac{\Omega_{\mathrm{ad}}[Q(t)]-\Omega_{\min}}{(\omega_e-\Omega_{\min})}, \tag{19}$$

where $\Omega_{\min}=\Omega_{\mathrm{ad}}(Q_{\min})$. This $X(t)$ function is usually approximated by a sum of several exponentials and should coincide with the relaxation function[34]

$$X(t)=\frac{1}{\pi E_r}\int_0^{\infty}\frac{J(\omega)}{\omega}\cos(\omega t)d\omega. \tag{20}$$

For $(Q-\Delta G)^2 \gg V_{\mathrm{el}}^2$, an approximate solution of Eq. (19) is given by

$$Q(t)\simeq Q_{\min}+(\omega_e-\Omega_{\min})X(t). \tag{21}$$

The use of $Q(t)$ described by Eq. (21) and of $\delta(t)=[1-AX^2(t)]$ for the calculations of the wave packet propagation implies that the anharmonicity of the excited free energy surface is neglected. The nonequilibrium rate constant $k(t)$ has been numerically shown to depend only weakly on the initial width $\delta(0)$, therefore this form of $\delta(t)$ is also used for calculating the CR kinetics with the anharmonic excited term. Moreover, $k(t)$ depends only weakly on whether $Q(t)$ is determined by Eqs. (19) or (21).

It is well known that an exponential decay of $X(t)$ leads to a Debye-like spectral density $J(\omega)$, but an instant velocity does not exist in this model, and as a result, the integral in Eq. (12) is divergent. For this reason, the Brownian oscillator model for which the spectral density is given by Eq. (22),[27]

$$J(\omega)=\frac{2E_r\gamma\Omega^2\omega}{(\omega^2-\Omega^2)^2+\omega^2\gamma^2} \tag{22}$$

is used. When the friction coefficient of the reaction coordinate $\gamma$ is zero, the oscillator experiences a coherent motion at the frequency $\Omega$. In the strong overdamped limit, $\gamma \gg \Omega$, the behavior of the Brownian oscillator becomes close to Debye-type with a relaxation time $\tau_r=\gamma/\Omega^2$, except in the short time region where $t<1/\gamma$.[28]

Real solvents are usually characterized by several relaxation time scales. In this case, the spectral density $J(\omega)$ can be well reproduced by a sum of Brownian oscillator spectral densities. Each individual density describes a vibrational mode with the parameters $\gamma_i$, $\Omega_i$, and $E_{ri}$, where $\tau_{ri}=\gamma_i/\Omega_i^2$ and $E_{ri}$ are the relaxation time and reorganization energy of $i$th mode, respectively, and $E_r=\Sigma_i E_{ri}$ is the total reorganization energy. In this case Eq. (20) gives $X(t)=\Sigma x_i e^{-t/\tau_{ri}}$ with $x_i=E_{ri}/E_r$.

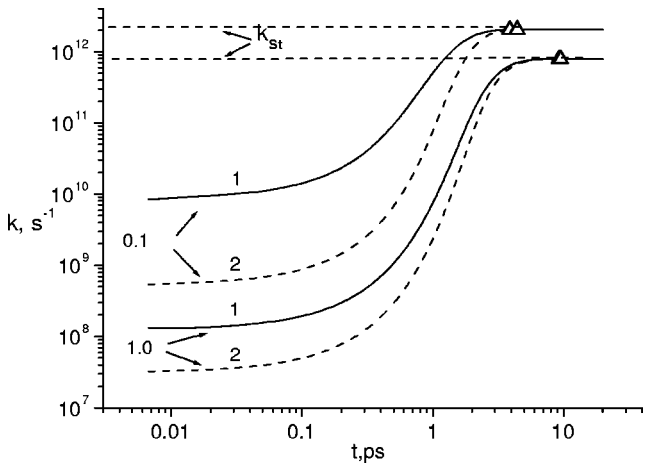


FIG. 2. Time dependence of the CR reaction rate (single mode model). The parameters used are: $T=300$ K, $\tau_e=50$ fs, $V_{\mathrm{el}}=0.1$ eV, $E_r=1.0$ eV, $\gamma=0.2$ eV, and $\tau_r=1$ ps. The numbers near the curves are the $-\Delta G$ values in electron volts. The solid and dashed curves correspond to the excitation frequency at $\omega_e^+$ and $\omega_e^-$, respectively.

## IV. RESULTS AND DISCUSSION

The results of the numerical calculations of the nonequilibrium CR rate $k(t)$ are presented in Fig. 2 for a model including a single relaxation time and in Fig. 3 for a model with two relaxation times. For CR reactions in strongly polar solvents (acetonitrile, alcohols, and others), the relaxation times $\tau_{r1}$ and $\tau_{r2}$ lie typically in the 0.1–1 ps and 5–10 ps ranges, respectively.[35–37] Such time scales have been used in the calculations. The ''triangle,'' ''star,'' and ''circle'' symbols in Figs. 2 and 3 indicate the time at which the excited adiabatic state population decreases by a factor 100. It can be

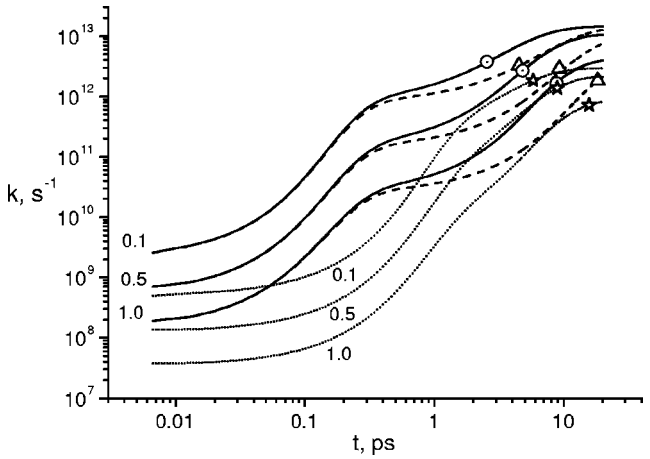


FIG. 3. Time dependence of the CR reaction rate (two mode model). The parameters used are: $T=300$ K, $\tau_e=50$ fs, $V_{\mathrm{el}}=0.1$ eV, $E_{r1}=0.7$ eV, $E_{r2}=0.3$ eV, and $\gamma=0.2$ eV. $\tau_{r1}=0.1$ ps, $\tau_{r2}=10$ ps (solid curves); $\tau_{r1}=0.1$ ps, $\tau_{r2}=5$ ps (dashed curves); $\tau_{r1}=0.5$ ps, $\tau_{r2}=5$ ps (dotted curves). The $-\Delta G$ values in electron volts are indicated near the curves.

easily seen that vibrational nonequilibrium leads to a strongly nonexponential CR dynamics on the whole experimentally observable time window.

The time dependencies of the rate reflect the propagation of the wave packet from its initial position towards the excited state free energy minimum (see Fig. 1). Because the transition rate between the adiabatic states is inversely proportional to the energy gap, the wave packet motion results in an increase of the rate.

In the single relaxation time model, the exponential stage of the excited population decay occurs only after a time delay of the order of the relaxation time scale, $t \sim \tau_r$, when $k(t)$ is just approaching to $k_{st}$ (Fig. 2). In this case, the ultrafast stage of the CR dynamics, i.e., when $t < \tau_r$, is thus strongly nonexponential. An increase of the electronic coupling $V_{el}$ leads to a decrease of the rate and to a weaker contribution of nonequilibrium CR dynamics. As a consequence, the nonexponentiality of the CR kinetics is less pronounced. In the Marcus inverted region, the population decay slows down with increasing driving force and thus the dynamics goes toward the exponential regime.

In the two mode model, the behavior of $k(t)$ is essentially the same as in the single mode model as long as the inequality $\tau_{r2}/\tau_{r1} < 10$ holds (see the dotted curves in Fig. 3). However, if the difference between the relaxation time scales is larger, $k(t)$ exhibits a plateau between $\tau_{r2}$ and $\tau_{r1}$ (see the nearly horizontal part of solid and dashed curves in Fig. 3). Obviously, the left edge of the plateau corresponds to the time at which the relaxation of the fast mode is practically over, while the right edge coincides with onset of the slower mode motion. It should be emphasized that the plateau can in principle coincide with the experimentally observable time window. In this case, the CR reaction is over before the relaxation of the slower mode has actually started.

### A. Excited state population dynamics

The excited state population $P_e(t)$ is determined with the time dependent rate Eq. (11) as

$$P_e(t) = \exp\left\{ -\int_0^t k(t')dt' \right\}. \tag{23}$$

The nonexponential decay of the excited state population can be quantitatively reproduced by a function of the form

$$P_e(t) = \exp[-(t/\tau)^s]. \tag{24}$$

The parameter $s$ can be interpreted as a measure of the nonexponentiality of the decay. Values of $s > 1$ correspond to an increase of the rate with time and $s < 1$ to a decrease.

The $s$ and $\tau$ values obtained from the fit of Eq. (24) to the simulated data are listed in Table I. Several features can be observed:

(1) Within the framework of the adiabatic perturbation theory, the value of $s$ is predicted to be larger than unity in the whole range of parameters; this is a direct demonstration of the increase of the rate with time.

(2) The parameter $s$ decreases with increasing electronic coupling $V_{el}$ and increases with the carrier frequency of the pump pulse.

TABLE I. Parameters obtained from the fit of Eq. (24) to the calculated decay dynamics of the excited DAC population at the time interval after which 90% of the initial excited state population has decayed. The parameters used are: $E_{r1}=0.7$ eV, $E_{r2}=0.3$ eV, $\tau_{r1}=0.1$ ps, $\tau_{r2}=10$ ps, $\eta=+$, and $\eta=-$ correspond to the excitation frequency at half the absorption maximum on the high- and low-frequency sides, respectively. $k_{ef}$ is the effective rate constant. $R$ is the coefficient of correlation.

| $\eta$ | $\Delta G$(eV) | $V_{el}$(eV) | $s$ | $\tau$(ps) | $k_{ef}$(ps$^{-1}$) | $R^2$ |
|---|---|---|---|---|---|---|
| + | −0.5 | 0.1 | 1.74 | 3.33 | 0.225 | 0.998 |
| − | −0.5 | 0.1 | 1.52 | 5.19 | 0.412 | 0.998 |
| + | −0.5 | 0.4 | 1.29 | 10.44 | 0.104 | 0.999 |
| − | −0.5 | 0.4 | 1.17 | 8.81 | 0.120 | 0.999 |
| + | −1.0 | 0.1 | 2.37 | 7.62 | 0.109 | 0.997 |
| − | −1.0 | 0.1 | 1.84 | 5.19 | 0.148 | 0.997 |
| + | −1.0 | 0.4 | 1.46 | 18.61 | 0.057 | 0.999 |
| − | −1.0 | 0.4 | 1.31 | 16.41 | 0.064 | 0.999 |
| + | −1.5 | 0.1 | 2.75 | 22.47 | 0.050 | 0.998 |
| − | −1.5 | 0.1 | 2.41 | 19.93 | 0.056 | 0.998 |
| + | −1.5 | 0.4 | 1.41 | 36.78 | 0.023 | 0.999 |
| − | −1.5 | 0.4 | 1.32 | 34.37 | 0.025 | 0.999 |

(3) The dependence of $s$ on the reaction free energy $\Delta G$ is not monotonous. In the free energy range presented in Table I, namely $-\Delta G < 1.5$ eV, $s$ increases with $-\Delta G$. In the larger driving force regime, the reaction is considerably slower and thus nonthermal CR plays a minor role. In this case, the magnitude of $s$ should decrease and approach unity.

(4) A variation of the carrier pulse frequency from one half maximum of the absorption band to the other alters the magnitude of $s$ by 10%–30%.

### B. Spectral effect

In order to quantify the decay of the excited state population, a time-independent effective rate constant $k_{ef}$ is used

$$k_{ef}^{-1}(\omega_e) = \int_0^\infty \exp\left\{ -\int_0^{t_1} k(t_2)dt_2 \right\} dt_1. \tag{25}$$

The free energy dependencies of $k_{ef}(\omega_e)$ for the single and two mode models at a given $\omega_e$ are shown in Fig. 4. Neither

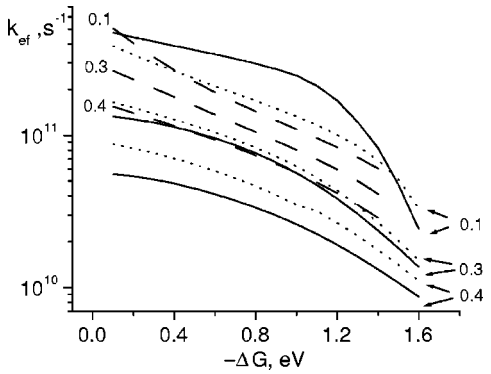


FIG. 4. Dependence of the effective rate on the CR free energy $\Delta G$. The parameters used are: $T=300$ K, $\tau_e=50$ fs, $E_{r1}=0.7$ eV, $E_{r2}=0.3$ eV, and $\gamma=0.2$ eV. The solid curves correspond to the model including a single relaxation time $\tau_r=1$ ps; the dashed and dotted curves correspond to the two mode model. $\tau_{r1}=0.1$ ps, $\tau_{r2}=10$ ps (dashed curves); $\tau_{r1}=0.5$ ps, $\tau_{r2}=5$ ps (dotted curves). The $V_{el}$ values in electron volts are indicated near the curves.

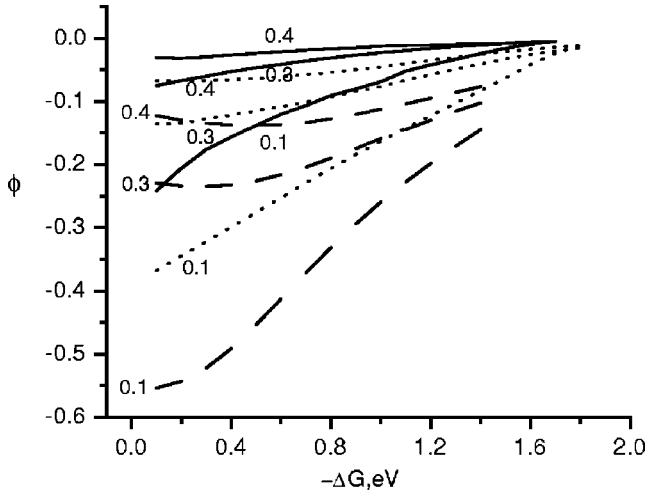


FIG. 5. Spectral effect $\phi$ as a function of CR free energy $\Delta G$. The solid curves correspond to the model including a single relaxation time $\tau_r = 1$ ps. The dashed and dotted curves correspond to the model with two relaxation times: $E_{r1}=0.7$ eV, $E_{r2}=0.3$ eV, $\gamma=0.2$ eV; $\tau_{r1}=0.1$ ps, $\tau_{r2}=10$ ps (dashed curves); $\tau_{r1}=0.5$ ps, $\tau_{r2}=5$ ps (dotted curves). The $V_{\mathrm{el}}$ values in electron volts are indicated near the curves.

the effective rate nor the stationary rate[8] exhibit the Marcus normal behavior, namely, an increase of the rate constant with increasing driving force. The magnitude of $k_{\mathrm{ef}}(\omega_e)$ is sensitive to the time scales of the reaction coordinate relaxation. Moreover, at a fixed relaxation time the effective rate rises with the friction coefficient $\gamma$.

The magnitude of the spectral effect is defined as

$$\phi = \frac{k_{\mathrm{ef}}(\omega_e^+) - k_{\mathrm{ef}}(\omega_e^-)}{k_{\mathrm{ef}}(\omega_e^-)}, \tag{26}$$

where $\omega_e^+$ and $\omega_e^-$ are the frequencies at half maximum of the charge transfer band ($\omega_e^+ > \omega_e^-$). Figure 5 shows the dependence of the spectral effect on $\Delta G$ for various values of the electronic coupling $V_{\mathrm{el}}$. For the models considered here, the spectral effect is always negative, namely, $k_{\mathrm{ef}}$ decreases with increasing excitation frequency $\omega_e$. It should be emphasized that the spectral effect becomes larger when the difference of relaxation time scales increases (dashed curves in Fig. 5).

The spectral effect is more pronounced in the low exergonicity regime, where the rate is maximal and the reaction is finished before the excited state population has reached thermal equilibrium. This is an additional evidence of the vibrational nonequilibrium origin of the spectral effect. The negative sign of the spectral effect can be explained as follows. The larger the frequency of the pump pulse, the farther from the excited state minimum the wave packet is initially prepared and, as a consequence, the larger the free energy gap for the nonradiative transition. As the rate depends inversely on the gap, a higher excitation frequency implies a slower rate. An increase of the driving force leads to a slowing down of the reaction and thus to a smaller contribution of the nonequilibrium stage of the reaction. For transitions between the adiabatic states, this picture does qualitatively not depend on the number of vibrational modes.

The calculations have only been performed within the interval $0.5\ \mathrm{eV} > V_{\mathrm{el}} > 0.1\ \mathrm{eV}$, where the effect is shown to be large enough to be experimentally observable by ultrafast spectroscopy. It is worth mentioning that the extrapolation of these results to smaller $V_{\mathrm{el}}$ values is limited by the conditions of applicability of the method used.

## V. CONCLUSION

The calculations presented in this paper have shown that, in the limit of strong electronic coupling, the vibrational nonequilibrium created by a short pump pulse leads, in general, to strongly nonexponential CR dynamics. Nevertheless, the system can exhibit nearly exponential CR kinetics in a sufficiently wide time window, if the relaxation time scales differ largely.

The spectral effect is another manifestation of vibrational nonequilibrium. In the case of strong electronic coupling, the spectral effect is always negative and occurs mainly in the low exergonicity regime. Its magnitude decreases sharply with increasing electronic coupling and almost vanishes for $V_{\mathrm{el}}$ larger than 0.5 eV. This implies that experimental investigations of the spectral effect, especially in the low exergonicity region, could allow an estimation of the magnitude of electronic coupling.

In the case of weak electronic coupling, namely when the transition occurs between the diabatic states, the spectral effect in the low exergonic region has been recently predicted to be positive if the medium polarization relaxation exhibits two or more relaxation time scales.[19,20] For this reason, the experimental investigations of the spectral effect in DACs could provide an insight into the ET reaction mechanism, in particular, to distinguish between adiabatic and diabatic pathways of the CR reaction.

Until now, only a very few experimental investigations of the spectral effect on DACs have been reported.[18,19] In the first of them, some indications of a negative spectral effect could be obtained.[18] More recently, strongly nonexponential CR dynamics that could be reproduced by Eq. (24) has been reported.[19] Moreover, a clear negative spectral effect was observed with one of the two DACs investigated. On the other hand, a slightly positive, close to zero, spectral effect was observed with the other complex. The origin of these two different behaviors has not been elucidated, but might be related to different electronic coupling.

In this paper, the decay dynamics of the population of the excited adiabatic state has been investigated. This decay was identified with CR. In reality in the normal region, $-\Delta G < E_r$, the ground adiabatic curves may consist of two wells. One well, the left one in Fig. 1, mainly corresponds to the charge transfer state, while the other one is the original neutral configuration of the system. In general, the excited adiabatic state relaxes to both ground state wells and, obviously, the electronic transition is followed by vibrational thermalization leading to thermal equilibration of the populations of the two wells. Charge recombination and the reverse process, charge separation, can also occur during this stage. If the barrier between the wells is large enough, these processes will take place on considerably slower time scales

than that of the nonadiabatic electronic transitions. Total CR dynamics may therefore differ substantially from the decay dynamics of the excited adiabatic state.

However, vibrational relaxation in the ground adiabatic state only gives a substantial contribution to CR dynamics in the free energy area close to zero. An increase of both the driving force and the electronic coupling lowers the potential barrier height between the wells and results in a decrease of the initial population of the well corresponding to the charge transfer state. Moreover, with a reorganization energy of $E_r = 1$ eV, it follows from Eqs. (13) and (16) that the potential barrier disappears completely in the region of parameters $\Delta G < -0.5$ eV and $V_{el} > 0.1$ eV. In such a case, the effect of vibrational relaxation of the adiabatic ground state on CR dynamics is insignificant. For real DACs investigated, the free energy is definitely smaller than $-0.5$ eV and this is one of the reasons why this second stage was not considered in the paper.

The second question connected with this problem is what is monitored in corresponding experiments. As a rule, a time-dependent absorption of an ionic state of one of the component of the DAC is measured. Most probably, for tightly composed DACs with large electronic coupling it implies that experimental signal reflects the adiabatic excited state decay.

## ACKNOWLEDGMENT

This work was supported by the Russian foundation for basic research grants (Grant Nos. 02-03-32275 and 04-03-96502).

[1] T. Asahi and N. Mataga, J. Phys. Chem. **95**, 1956 (1991).
[2] H. Segawa, C. Takehara, K. Honda, T. Shimidzu, T. Asahi, and N. Mataga, J. Phys. Chem. **99**, 503 (1992).
[3] S. M. Hubig, T. M. Bockman, and J. K. Kochi, J. Am. Chem. Soc. **118**, 3842 (1996).
[4] O. Nicolet and E. Vauthey, J. Phys. Chem. A **106**, 5553 (2002).
[5] M. Tachiya and S. Murata, J. Am. Chem. Soc. **116**, 2434 (1994).
[6] L. D. Zusman, Chem. Phys. **49**, 295 (1980).
[7] B. I. Yakobson and A. I. Burshtein, Chem. Phys. **49**, 385 (1980).
[8] P. A. Frantsuzov and M. Tachiya, J. Chem. Phys. **112**, 4216 (1999).
[9] A. I. Shushin, Chem. Phys. **60**, 149 (1981).
[10] R. D. Coalson, D. G. Evans, and A. Nitzan, J. Chem. Phys. **101**, 436 (1994).
[11] M. Cho and R. J. Silbey, J. Chem. Phys. **103**, 595 (1995).
[12] W. Domcke and G. Stock, Adv. Chem. Phys. **100**, 1 (1997).
[13] J. M. Jean, J. Phys. Chem. A **102**, 7549 (1998).
[14] D. Egorova, M. Thoss, W. Domcke, and H. Wang, J. Chem. Phys. **119**, 2761 (2003).
[15] K. Ando and H. Sumi, J. Phys. Chem. B **102**, 10991 (1998).
[16] K. Wynne and R. M. Hochstrasser, Adv. Chem. Phys. **107**, 263 (1999).
[17] G. C. Walker, E. Akesson, A. E. Johnson, N. E. Levinger, and P. F. Barbara, J. Phys. Chem. **96**, 3728 (1992).
[18] O. Nicolet, A. Ivanov, and E. Vauthey, in *Femtochemistry and Femtobiology: Ultrafast Events in Molecular Science*, edited by J. T. Hynes and M. Martin (Elsevier, Amsterdam, 2004), p. 331.
[19] R. G. Fedunov, S. V. Feskov, A. I. Ivanov, O. Nicolet, S. Pagès, and E. Vauthey, J. Chem. Phys. **121**, 3643 (2004).
[20] A. I. Ivanov, F. N. Belikeev, R. G. Fedunov, and E. Vauthey, Chem. Phys. Lett. **372**, 73 (2003).
[21] E. Akesson, G. C. Walker, and P. F. Barbara, J. Chem. Phys. **95**, 4188 (1991).
[22] K. Tominaga, D. A. V. Kliner, A. E. Johnson, N. E. Levinger, and P. F. Barbara, J. Chem. Phys. **98**, 1228 (1993).
[23] I. V. Rubtsov and K. Yoshihara, J. Phys. Chem. A **101**, 6138 (1997).
[24] W. Jarzeba, S. Murata, and M. Tachiya, Chem. Phys. Lett. **301**, 347 (1999).
[25] E. Vauthey, J. Phys. Chem. A **105**, 340 (2001).
[26] E. E. Nikitin, *Theory of Elementary Atomic and Molecular Processes in Gases* (Clarendon, Oxford, 1974).
[27] A. Garg, J. N. Onuchic, and V. Ambegoakar, J. Chem. Phys. **83**, 4491 (1985).
[28] S. Mukamel, *Principles of Nonlinear Optical Spectroscopy* (Oxford University Press, New York, 1995).
[29] A. I. Ivanov and V. V. Potovoi, Chem. Phys. **247**, 245 (1999).
[30] P. A. Frantsuzov, S. F. Fischer, and A. A. Zharikov, Chem. Phys. **241**, 95 (1997).
[31] P. A. Frantsuzov, J. Chem. Phys. **111**, 2075 (1998).
[32] L. D. Zusman and A. B. Helman, Opt. Spectrosc. **53**, 248 (1982).
[33] B. Bagchi, D. W. Oxtoby, and G. R. Fleming, Chem. Phys. **86**, 25 (1984).
[34] G. Van der Zwan and J. T. Hynes, J. Phys. Chem. **89**, 4181 (1985).
[35] M. L. Horng, J. A. Gardecki, A. Papazyan, and M. Maroncelli, J. Phys. Chem. **99**, 17311 (1995).
[36] T. Joo, Y. Jia, J.-Y. Yu, M. J. Lang, and G. R. Fleming, J. Chem. Phys. **104**, 6089 (1996).
[37] J.-C. Gumy and E. Vauthey, J. Phys. Chem. A **104**, 10737 (1999).